BMC Biotechnology

RESEARCH

Open Access

Recombinant hirudin and PAR-1 regulate macrophage polarisation status in diffuse large B-cell lymphoma

Qiang Pei[1,2,3*], Zihui Li[1,2,4], Jingjing Zhao[1,2,4], Haixi Zhang[1,2,3], Tao Qin[1,2,3] and Juan Zhao[1,2,3]

Abstract

Background Diffuse large B-cell lymphoma (DLBCL) is a malignant tumour. Although some standard therapies have been established to improve the cure rate, they remain ineffective for specific individuals. Therefore, it is meaningful to find more novel therapeutic approaches. Macrophage polarisation is extensively involved in the process of tumour development. Recombinant hirudin (rH) affects macrophages and has been researched frequently in clinical trials lately. Our article validated the regulatory role of rH in macrophage polarisation and the mechanism of PAR-1 by collecting clinical samples and subsequently establishing a cellular model to provide a scientifically supported perspective for discovering new therapeutic approaches.

Method We assessed the expression of macrophage polarisation markers, cytokines and PAR-1 in clinical samples. We established a cell model by co-culture with THP-1 and OCI-Ly10 cell. We determined the degree of cell polarisation and expression of validation cytokines by flow cytometry, ELISA, and RT-qPCR to confirm the success of the cell model. Subsequently, different doses of rH were added to discover the function of rH on cell polarisation. We confirmed the mechanism of PAR-1 in macrophage polarisation by transfecting si-PAR-1 and pcDNA3.1-PAR-1.

Results We found higher expression of M2 macrophage markers (CD163 + CMAF+) and PAR-1 in 32 DLBCL samples. After inducing monocyte differentiation into M0 macrophages and co-culturing with OCI-Ly10 lymphoma cells, we found a trend of these expressions in the cell model consistent with the clinical samples. Subsequently, we discovered that rH promotes the polarisation of M1 macrophages but inhibits the polarisation of M2 macrophages. We also found that PAR-1 regulates macrophage polarisation, inhibiting cell proliferation, migration, invasion and angiogenic capacity.

Conclusion rH inhibits macrophage polarisation towards the M2 type and PAR-1 regulates polarisation, proliferation, migration, invasion, and angiogenesis of DLBCL-associated macrophages.

Keywords Diffuse large B-cell lymphoma, Macrophage polarisation, Recombinant hirudin, PAR-1

*Correspondence:
Qiang Pei
peiqiang828@163.com
[1]Department of Hematology, The First People's Hospital of Yunnan Province, No. 157 of Jinbi Street, Kunming, 650032 Yunnan, China
[2]Affiliated Hospital of Kunming University of Science and Technology, Kunming, 650032 Yunnan, China
[3]Yunnan Province Clinical Center for Hematologic Disease, Yunnan, China
[4]Medical School, Kunming University of Science and Technology, Kunming, 650500 Yunnan, China

Introduction

Non-Hodgkin's lymphoma (NHL) is a haematological malignancy, of which diffuse large B-cell lymphoma (DLBCL) is one of the prevalent subtypes [1]. Chemotherapy with rituximab is currently a standard and effective treatment. The article has shown that patients who receive rituximab treatment have an overall survival rate of approximately 65% in five years [2]. Despite the ability of this chemotherapy modality to improve patient prognosis, abnormalities in the tumour microenvironment continue to influence the progression of DLBCL [3]. Consequently, it is imperative to explore additional therapeutic options related to cell mechanisms, including T-cells, macrophages, stromal cells, and other tumour microenvironmental cells for DLBCL diagnosis and treatment.

Macrophages are derived from mononuclear phagocytes, which have strong heterogeneity and plasticity. They can participate in the organism's immune regulation. The polarisation state of macrophages in different microenvironments has different regulatory functions on diseases [4]. As the article states, osteoclasts originate from macrophages, which regulate the differentiation of osteoblasts and participate in the processes of bone injury, healing, and so on, during the process of bone injury [5]. In the central nervous system, there are different types of macrophages, including microglia, and the classification of the polarisation state of macrophages correlates with the activation state of microglia [6]. Macrophages exhibit different activation states in response to changes in the microenvironment. This is also referred to as macrophage polarisation. Macrophages are divided into two more typically polarised states, M1 (classically activated) and M2 (alternatively activated) [7]. M1 macrophage activation elicits an adaptive immune response and releases pro-inflammatory cytokines such as Th1 cytokines tumour necrosis factor (TNF)-α, interleukin-6 (IL-6) and IL-1β. M2 macrophages release the anti-inflammatory factors IL-10, TGF-β and Arginase (Arg) during activation, contributing to wound healing [8]. The imbalance between M1 and M2 is recognised as a causative factor in diseases such as cancer [9], cardiovascular diseases [10], liver diseases [11], and neurodegeneration [12]. Studies have illustrated that macrophages infiltrating the tumour microenvironment are related to poor cancer prognosis [13]. This type of cell is known as tumour-associated macrophage (TAM), which promotes the proliferation and migration of tumour cells [14]. M2 macrophage is tumour-resistant and immunosuppressive [15], and the study of the role of M2 macrophages in cancer has been recognised in a large number of articles. miRNA-induced polarisation of M2 macrophages promotes metastasis in colorectal cancer [16]. In ovarian cancer, treatment by targeting M2 macrophage polarisation has modulated chemoresistance in patients [17]. LncRNA can promote breast cancer development and metastasis by increasing M2 macrophage polarisation [18]. These studies investigated approaches that can mediate cancer therapy from the perspective of M2 macrophages. Although there have been articles discussing the transcriptomic profiles of macrophages in DLBCL [19], as well as advances in novel chemotherapeutic approaches based on macrophage polarisation in DLBCL [20], the treatments remain chemoresistant. Therefore, the discovery of promising macrophage polarisation-based therapies in DLBCL still requires more exploration.

The process of cancer progression and blood clots are strongly linked. Thrombin promotes angiogenesis and the growth of cancer cells. Numerous studies have demonstrated that thrombin binds with the protease-activated receptor-1 (PAR-1) to promote tumour metastasis. For example, thrombin stimulating PAR-1 mediates the progression of breast cancer [21, 22] and melanoma [23]. PAR-1 is linked to distant metastasis and overall survival of kidney cancer cells [24]. The effect of chemicals on thrombin was explored in a clinical study in lymphoma [25]. However, the number of studies on thrombin and especially PAR-1 in DLBCL is insufficient. Although, drugs that clinically target PAR-1 include Vorapaxar, Atopaxar hydrobromide, etc. [26], there is still a need for more evidence for PAR-1 inhibitors in cancer. In recent studies, we have found rH to be a promising therapeutic modality. Hirudin has been used as an anticoagulant, and recombinant hirudin (rH), an inhibitor with a potent coagulation effect, has been shown to inhibit the proliferation and metastasis of a wide range of cancer cells with rH. In a mouse model of prostate cancer, it has been shown to inhibit metastasis of transplanted tumours following the addition of rH [27]. Studies have demonstrated that in certain types of cancer, such as lung cancer [28] and laryngeal cancer [29], rH can inhibit the proliferation and spread of cancerous cells. rH has been shown to mediate macrophage polarisation to regulate vascular function in chronic renal failure [30]. Thus, we inferred that rH was able to regulate macrophage polarisation. There have been several studies on rH and PAR-1 demonstrating their key functions in disease. In ovarian cancer, rH effectively inhibited PAR-1, thereby suppressing tumour cell growth [31]. In non-small cell lung cancer, rH could be a potential therapeutic target as a novel ning degree inhibitor [32]. In clinical studies in NHL, it was demonstrated that the action of thrombin might be altered by the addition of rH [25]. Based on these backgrounds, we reasoned that rH could act as an inhibitor of PAR-1. Therefore, it is imperative to investigate the function of PAR-1 and rH in DLBCL. This study aimed to assess the functions of rH and PAR-1 in DLBLC and to investigate their mechanisms of action in TAM.

Methods and materials

Clinical samples

32 samples of DLBCL patients and the cancer-adjacent tissue were obtained from the First Affiliated Hospital of Yunnan Province. The samples were histopathologically identified and had available survival data. The study was reported to and approved by the First Affiliated Hospital Ethics Committee of Yunnan Province (Issue No. YYLH052). All pieces complied with medical ethical requirements, and informed consent was signed for information collection. The clinical sample information is shown in Supplementary Tables S1–S2.

Cell differentiation

In a Transwell system, OCI-Ly10 lymphoma cells (Chemicalbook, China) were purchased and co-cultured with the differentiated THP-1 cells. In the logarithmic growth phase, human mononuclear THP-1 cells (Abiowell, China) were incubated with Phorbol-12-myristate-13 acetate (PMA) for 48 h, then induced to differentiate into M0 macrophages. M1 macrophages were obtained after the addition of 100 nmol/L PMA, 100 ng/mL lipopolysaccharide (LPS) and 20 ng/mL IFN-γ cultured for 24 h. M2 macrophages were obtained by adding 100 nmol/L PMA, 20 ng/mL IL-4 and 20 ng/mL IL-13 after 48 h of culture [33, 34].

Cell culture and transfection

Human DLBCL cell line OCI-Ly10 cells were cultured in RPMI1640 medium containing 10% fetal bovine serum and 1% penicillin/streptomycin with 5% CO_2 at 37 °C. When cell fusion reached 80%, plasmids were transfected into the cells using Lipomine3000 (ThermolFisher, USA) and collected after 48 h. PAR-1-related plasmids were designed and synthesised by GenePharma (China).

RT-qPCR

Following the provided instructions, total RNA was taken from cultured cells and clinical sample tissues by TRIzol (Invitrogen). RNA was isolated using the kit (Yeasen, China). Total RNA was transcribed using a cDNA synthesis kit (ThermolFisher, USA). β-actin was used as an internal reference for normalisation. Results were determined by the dissolution curve and then calculated via the $2^{-\Delta\Delta Ct}$. The primer sequences are displayed in Table 1.

Table 1 The primer sequences of RT-qPCR

		Sequence Reversed 5′-3′
IL-6	GCGCGACCACCCCAGA	AGTGCAGGGTCCGAGGTATT
TNF-α	GAGGCCAAGCCCTGGTATG	CGGGCCGATTGATCTCAGC
IL-1β	AGCTACGAATCTCCGACCAC	CGTTATCCCATGTGTCGAAGAA
TGF-β	GGCCAGATCCTGTCCAAGC	GTGGGTTTCCACCATTAGCAC
Arg	AAAGCTGCGAGTCCTTGGTTA	CGGGATACAGGTCCGTGGTA
IL-10	TCAAGGCGCATGTGAACTCC	GATGTCAAACTCACTCATGGCT
β-actin	CCCTGGAGAAGAGCTACGAG	GGAAGGAAGGCTGGAAGAG

Immunohistochemistry (IHC)

The pathological tissue sections were preserved with 4% paraformaldehyde to prepare paraffin slices, and the sample tissues were continuously sliced for 4 μm, five consecutive sections were made of each sample tissue. After baking, the paraffin sections were dehydrated and antigenic repaired. The antibody-PAR-1 (Abcam, ab23374, 1:1000) was added and incubated at 37℃. Then, a DAB colour development solution (Beyotime, China) was used to develop tissue sections. Use ImageJ to count the expression of PAR-1 according to the method in the article [35].

Flow cytometry

Macrophages were blown repeatedly with a pipette gun to obtain a cell suspension. After PBS washing, centrifugation was performed at 500 g for 5 min. The supernatant was removed and 1×10^6 cells were taken and added to 100ul of PBS buffer, the antibodies CD68 (Abcam, ab192847, 1:100) and CD163 (Abcam, ab182422, 1:60) were added and incubated at room temperature. PBS was washed and detected by a flow cytometer (ThermolFisher, USA). For the detection of macrophage surface marker expression in tissues, 5 sections of each sample tissue were made and digested using trypsin according to the references [36], the treated cell suspension was filtered through nylon mesh and processed by centrifugation at 300 g afterwards and the supernatant was discarded. After being washed with PBS, it can be used for subsequent assays. Data processing was completed in FlowJo.

Enzyme-linked immunosorbent assay (ELISA)

The sample tissue was taken and transferred into a container. PBS were added and ground thoroughly, frozen, and thawed twice. The treated sample solution was centrifuged at 5000 g for 5 min, and the supernatant was taken for subsequent testing. For cell samples, the cell culture solution was centrifuged at 1000 g for 20 min, and then the supernatant was used for subsequent testing. The standards were diluted in proportion to the gradient according to the instructions. Then, the 50 μl of standards were added to each well separately. The criteria and samples were labelled with horseradish peroxidase (HRP). The assay plate was placed at 37 °C for 60 min. The concentrations of IL-6, TNF-α, IL-1β, IL-10, TGF-β and Arg were measured by ELISA kit (ThermolFisher, USA).

Western blotting

Cells were lysed using a configured RIPA protein lysate to extract the protein solution. The supernatant was collected by high-speed centrifugation at 4 °C for 3 min at a low temperature. Protein concentration was determined using an enzyme marker at an OD value 562, and the actual concentration of the sample was subsequently calculated by the method in the article [37]. Proteins were denatured by 100 °C heat, after which SDS-PAGE was added to separate the broken gel by electrophoresis and transferred to a PVDF membrane. When transferring the membrane finished, 5% skimmed milk was used for containment. The primary antibody was PAR-1 (Abcam, ab117749, 1:1000). GADPH was used as an internal reference protein. PVDF membrane cropped on the line before incubation with antibody. The original strips are shown in the Supplementary File.

5-Ethynyl-29-deoxyuridine (EDU)

Cells were inoculated into 24-well plates and incubated with 2ul of EDU (Ribobio, China) for 3 h. This was followed by paraformaldehyde fixation and staining following the manufacturer's guidelines.

Cell migration, invasion and angiogenesis assay

For Transwell assay, cells were inoculated into the upper chamber of the Transwell (Corning, USA) with medium without FBS at the bottom, the cell density was 5×10^5/ml. Then, medium, including PBS, was added to the lower chamber. Incubation was next performed for 24 h, and a cotton swab was used to scrape the cells mechanically from the upper chamber. At this time, cells migrating to the bottom were fixed by paraformaldehyde. After crystal violet staining, the cells were processed for counting using ImageJ. For wound healing assay, cells were seeded at same density into 6-well plates, when the cells were fused to more than 90%, cell scratches were created using the tip of a 200 μl pipette. Images were obtained by microscopy at 0 and 48 h, with 3 images obtained for each group. The wound width was measured and analysed by ImageJ. For angiogenesis experiments, 96-well plates were first pre-cooled until the matrix gel solidified (ACROBiosystems, China). The cells were digested and resuspended. The cell density was 2×10^5, cells were inoculated into the plate, and the 96-well plate was transferred to an incubator and incubated at 37 °C for 8 h. Tubular structures could be seen in any 3 fields of view in each well were observed and recorded at 100x. The photographs taken were quantitatively analysed using the ImageJ plug-in.

Database analysis

Correlations between genes and different macrophage types were analysed using TIMER 2.0. Differential expression of genes in DLBCL was analysed using GEPIA.

Statistical analysis

The statistics were provided as mean±SD (standard deviation). The differences between the two groups were compared by Students' t-tests. The statistical method of one-way analysis of variance (ANOVA) was used when comparing more groups, Tukey's multiple comparisons test was used. GraphPad Prism 8.0 software (GraphPad Software, Inc., USA) was used to analyse and visualise the data. Data represent replications of three independent experiments and have been described separately where different. $P<0.05$ means statistical significance.

Results

Polarisation of macrophages in clinical samples

We collected clinical information and pathological samples from 32 patients diagnosed with Diffuse large B-cell lymphoma (DLBCL) and tumour-adjacent specimens to determine the polarisation of macrophages in DLBCL. The expression of CD68+pSTAT1+cells (M1 macrophages) and CD163+CMAF+cells (M2 macrophages) was first examined in diseased and adjacent tissues. From the flow cytometry analysis, the positive rate of M1 macrophages decreased significantly in disease samples, while the opposite trend was for M2 macrophages (Fig. 1A, B). RT-qPCR was used for detecting the cytokines, and we found that IL-6, TNF-α and IL-1β expression was reduced in the disease samples, while IL-10, TGF-β and Arg expression increased (Fig. 1C). Subsequently, the expression level of PAR-1 was detected by IHC in the samples, and we found that PAR-1 was higher in DLBCL samples (Fig. 1D).

Effects of OCI-Ly10 lymphoma cells on macrophage activity and polarisation

To investigate the mechanism of tumour-associated macrophage (TAM), we first established a cellular model. We co-cultured OCI-Ly10 cells with human mononuclear THP-1 cells to study TAM activity and polarisation. As shown in the figure, human THP-1 cells, before induced differentiation, were in the form of suspended spheres. Compared with THP-1 cells, PMA-induced differentiated M0 macrophages showed adherent growth, gradually increased in size, were oval, and had a few pseudopods (Fig. 2A). The proportion of CD68+pSTAT1+and CD163+CMAF+positive cells in each group was detected by flow cytometry. We found that in the M0+OCI-Ly10 group, there were fewer CD68+pSTAT1+than in the M0. However, the opposite was for CD163+CMAF+, as demonstrated by a higher positivity rate in the M0+OCI-Ly10 group than in the M0 group (Fig. 2B). Subsequently, we tested the

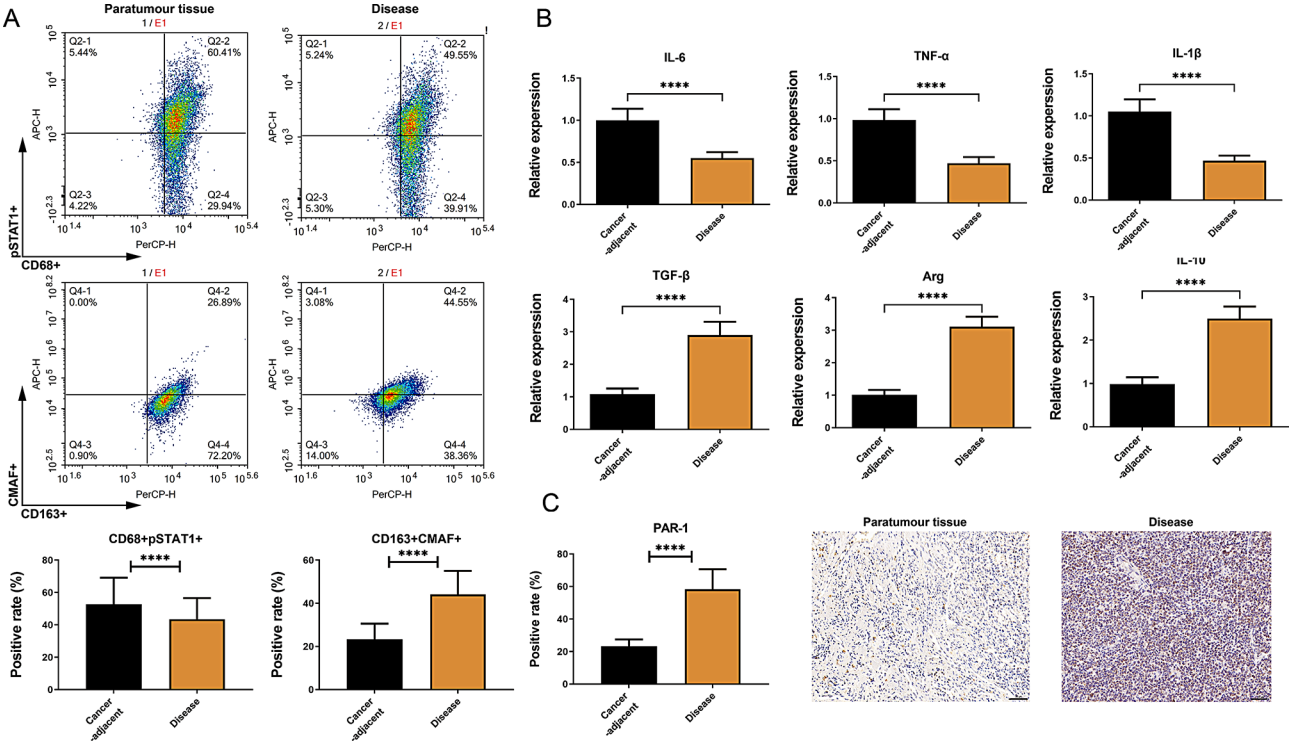

Fig. 1 Macrophage polarisation and PAR-1 expression in clinical samples. **A** CD68 + pSTAT1 + and CD163 + CMAF + were detected by flow cytometry. The supporting images of the gating strategy are shown in Supplementary Fig. S1A. **B** RT-qPCR for the expression of IL-6, TNF-α, IL-1β, IL-10, TGF-β and Arg. **C** Immunohistochemical (IHC) detection of PAR-1 expression in DLBCL tissue and adjacent tissue, scale bar = 50 μm, $n = 5$. A T-test was used to compare the two groups. ****$P < 0.0001$

concentrations and mRNA expressions of IL-6, TNF-α, IL-1β, IL-10, TGF-β and Arg in the supernatant of each group by ELISA (Fig. 2C) and RT-qPCR (Fig. 2D), respectively. It was found that they showed the same trend, and the concentration and expression of IL-6, TNF-α and IL-1β were lower in the M0 + OCI-Ly10 group than in the M0 group. While IL-10, Arg and TGF-β were higher in the experimental group than in the M0 group. These experiments indicated that our in vitro cellular models were established successfully, this was demonstrated by marked changes in cell morphology, a decrease in M1 macrophage markers and an increase in M2 markers, with the M0 + OCI-Ly10 group used to simulate TAMs.

Effect of recombinant hirudin (rH) on M0, M1 and M2 macrophage

To investigate the influence of rH on macrophages, we used the M0 + OCI-Ly10 co-culture system, and adjusted different concentrations of rH in each of the experimental groups. As could be seen from the experimental results of cck-8 (Fig. 3A), different concentrations of rH did not affect the viability of M0 macrophages. We subsequently added IL-4 and IL-13 for polarised M2 macrophages. LPS and IFN-γ were used to induce M1 macrophages. Flow cytometry showed a consistent trend for M1 and M2 macrophages. The proportion of CD68 + pSTAT1 + positive cells in the experimental group increased with increased rH concentration (Fig. 3B). However, the ratio of CD163 + CMAF + then decreased with the addition of rH (Fig. 3C). The statistics showed a significant difference (Fig. 3D). Then, we examined inflammatory factors' concentration and expression levels (Fig. 4A, B). The results of ELISA and RT-qPCR showed that the concentration and expression of IL-10, TGF-β, and Arg in M1 and M2 macrophages were decreased with increasing rH concentration compared to controls. Expression of IL-6, TNF-α, and IL-1β increased with increasing rH concentration compared to the control group. We also examined the expression of PAR-1, and the results of western blotting showed that after increasing the rH concentration, the expression of PAR-1 was reduced compared to the control (Fig. 4C). These findings showed that rH promoted the polarisation of M1 types but inhibited the polarisation of M2 macrophages and PAR-1.

Effects of PAR-1 on M2 macrophages

We selected M2 macrophages (IL-4/IL-13: +) transfected with sh-PAR-1 and pcDNA3.1-PAR-1 to verify how PAR-1 affects macrophage polarisation. Transfection efficiency was shown as western blotting results (Fig. 5A). Compared to control, CD68 + pSTAT1 + increased after

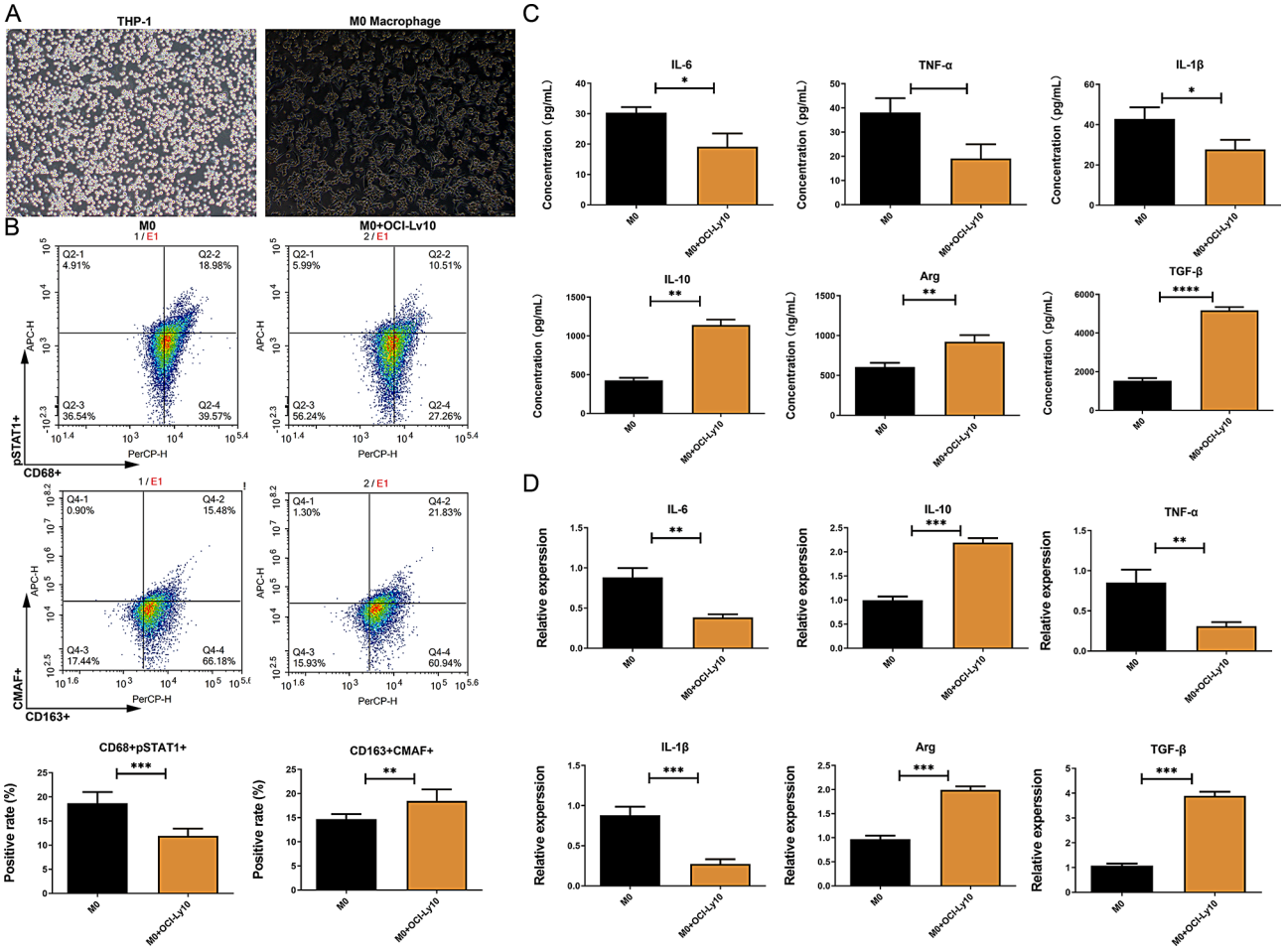

Fig. 2 Validation of marker and inflammatory factor expression in cellular models. **A** Cell morphology of monocyte THP-1 before and after induction by addition of 160 nmol/L PMA. **B** Flow cytometry revealed positive expression of CD68 + pSTAT1 + and CD163 + CMAF+. The supporting images of the gating strategy are shown in Supplementary Fig. S1B. **C** ELISA results showed the concentration of inflammatory cytokines in the different groups of macrophages. **D** RT-qPCR results showed the expression of IL-6, TNF-α, IL-1β, IL-10, TGF-β and Arg. A T-test was used to compare the two groups. ****$P < 0.0001$, ***$P < 0.001$, **$P < 0.01$ and *$P < 0.05$

the knockdown of PAR-1 and decreased after PAR-1 overexpression. However, CD163+CMAF+showed an opposite trend, with a decrease in the positive rate after transfection with sh-PAR-1 and an increase in the positive rate after transfection with pcDNA3.1-PAR-1 (Fig. 5B). The statistical results showed significant differences (Fig. 5C). We then examined the concentration and expression of inflammatory factors by ELISA and qPCR (Fig. 6A, B). The results of these two experiments consistently showed that knockdown of PAR-1 led to a decrease in IL-10, TGF-β, and Arg, and overexpression instead led to an increasing trend in them. IL-6, TNF-α, and IL-1β showed the opposite results, with knockdown of PAR-1 leading to an increase in their levels and overexpression of PAR-1 decreasing their levels. These results indicated that knockdown PAR-1 promotes the conversion of M2 macrophages to M1 macrophages.

Effect of PAR-1 on OCI-Ly cells

To further investigate the effects of PAR-1 on TAM, we used OCI-Ly10 lymphoma cells. We detected the cell viability by EDU, invasion by Transwell, and cell migration by wound healing and used angiogenesis assay after co-culture for calculating the blood vessel formation (Fig. 7A-D). The results showed that cell viability, migration index, cell number and tube number decreased after knockdown of PAR-1. However, after overexpression of PAR-1, these abilities were enhanced. The statistics showed significant differences (Fig. 7E). These results suggested that PAR-1 promotes lymphoma cells' proliferation, invasion, migration, and angiogenic capacity.

Discussion

Diffuse large B-cell lymphoma (DLBCL) is a typical and highly aggressive form of lymphoma. Although therapeutic approaches, such as CD20 monoclonal antibody

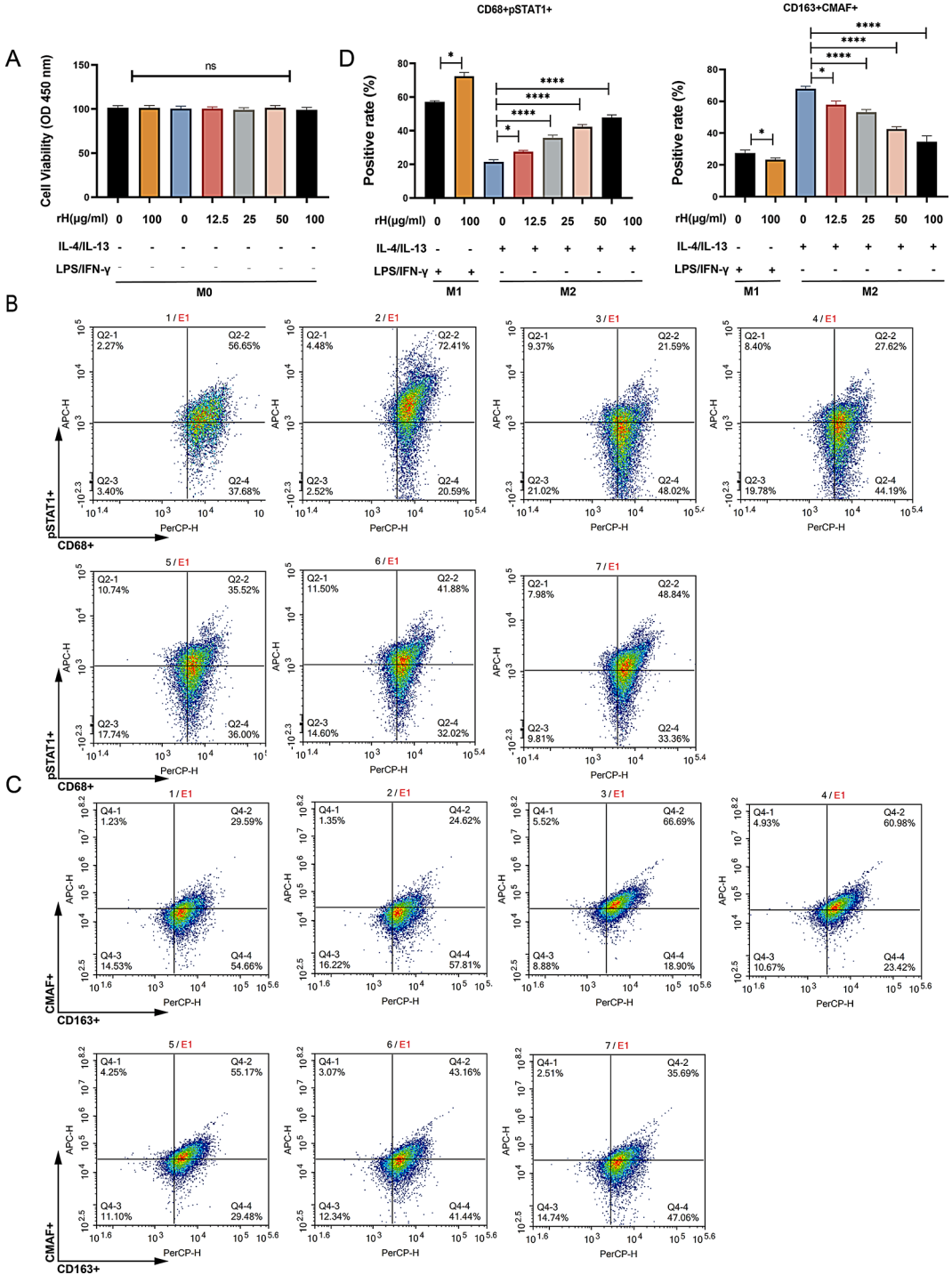

Fig. 3 The polarisation of the cell after the addition of rH. **A** CCk-8 showed that there was no fluctuation in the activity of the cells after the addition of different concentrations of rH. **B** The results of the flow cytometry assay showed a positive correlation between the positivity of CD68 + pSTAT1 + and the concentration of rH. The supporting images of the gating strategy are shown in Supplementary Fig. S1C. **C** The flow cytometry assay demonstrated a negative correlation between the doses of rH and the positivity of CD163 + CMAF+. The supporting images of the gating strategy are shown in Supplementary Fig. S1C. **D** Statistical results of marker positivity. One-way ANOVA was for comparison between more groups. n.s, not significant, ****$P < 0.0001$, and *$P < 0.05$

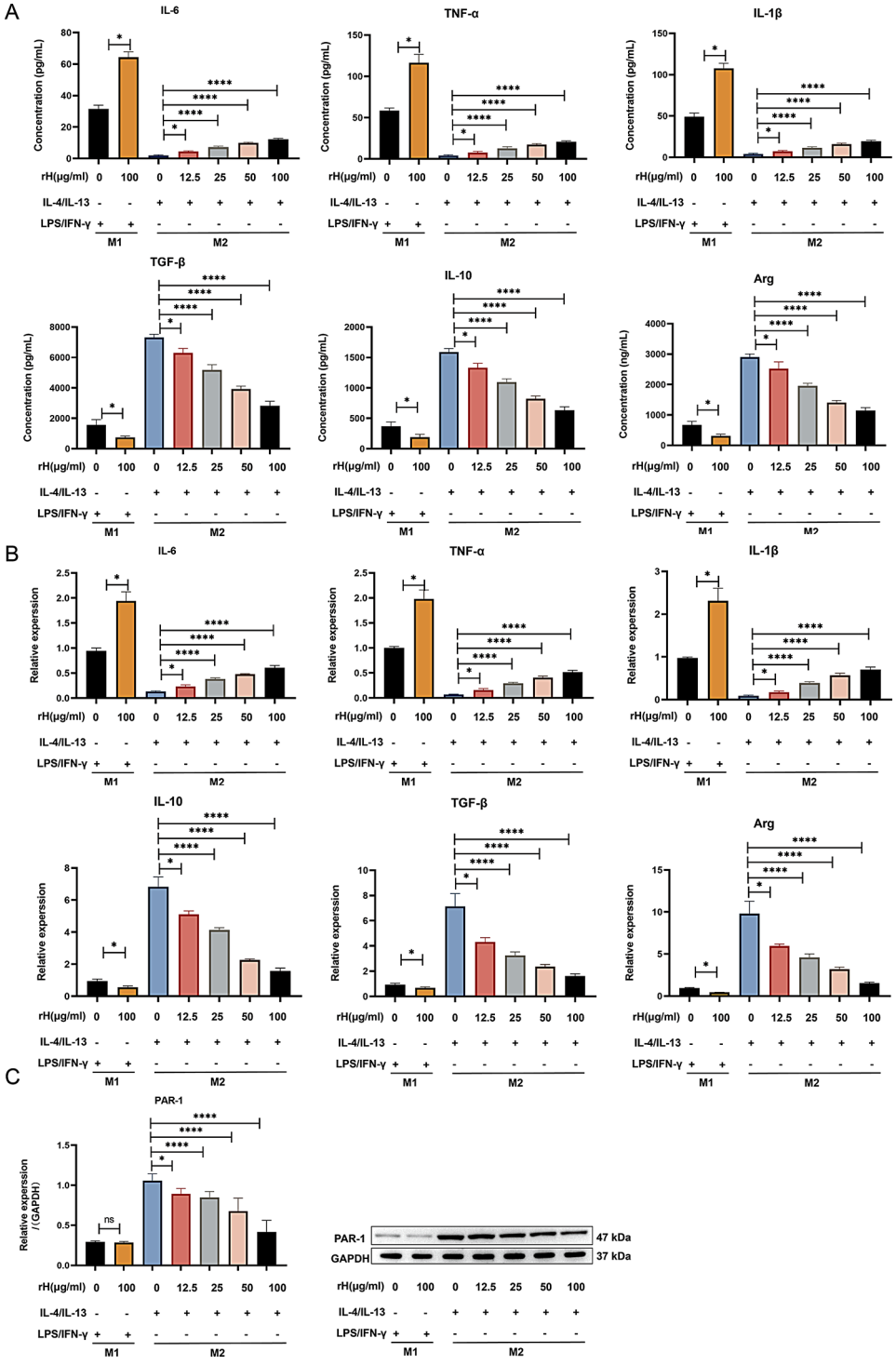

Fig. 4 Effects of different concentrations of rH on the concentration and expression of inflammatory factors and PAR-1. **A** The ELISA data displayed the concentration of cytokines in the various macrophage groups. **B** RT-qPCR showed the expression of inflammatory factors. **C** Western blotting expression showed that PAR-1 was affected by different concentrations of rH. The image showed a cropped blot, the original blot was included in the Supplementary file. One-way ANOVA was used for comparison between multiple groups. ****$P < 0.0001$ and *$P < 0.05$. n.s, not significant

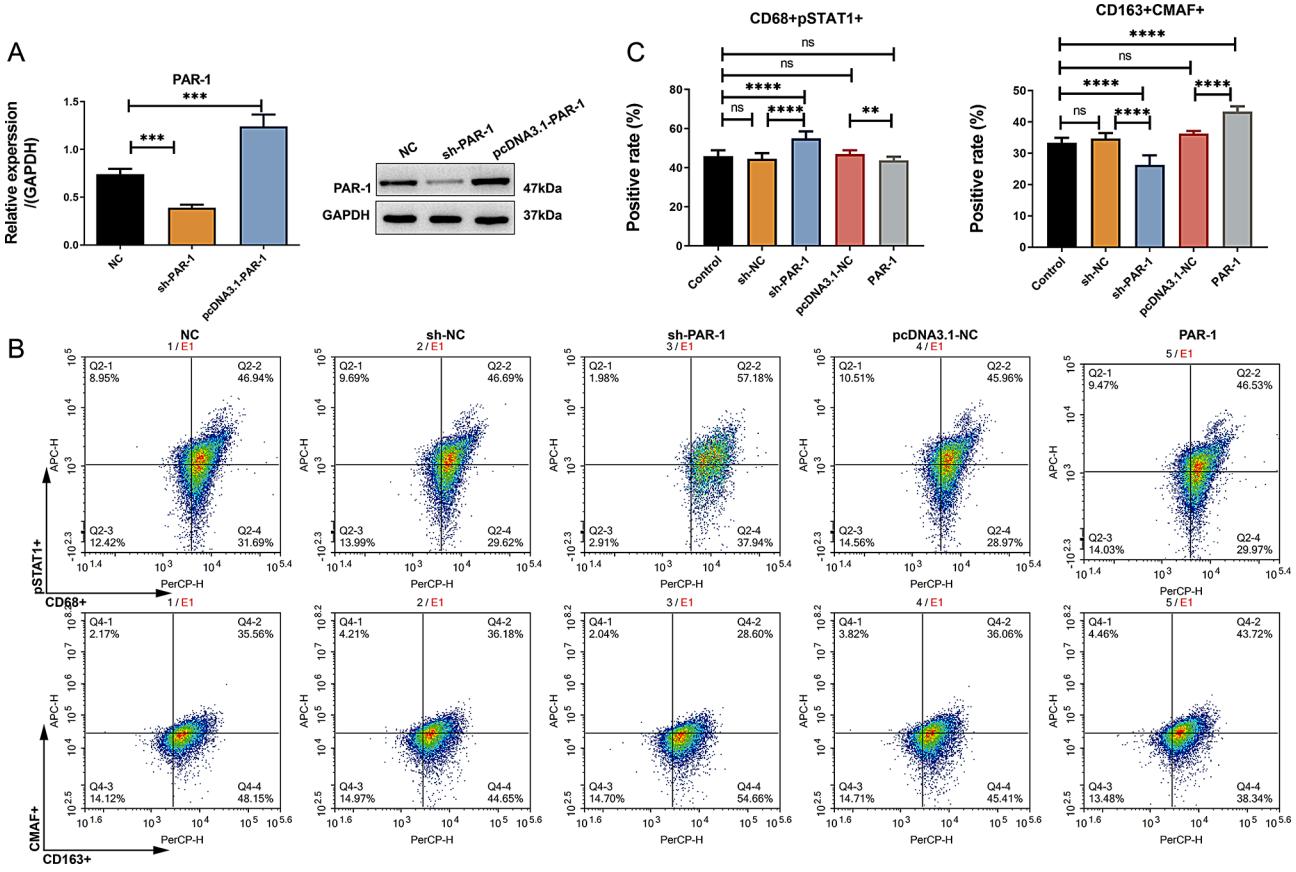

Fig. 5 Effect of knockdown and overexpression of PAR-1 on M2 macrophage. **A** Western blotting examined the efficiency of transfection of sh-PAR-1 and pcDNA3.1-PAR-1. The image showed a cropped blot, the original blot was included in the Supplementary file. **B** Effect on cell polarisation after transfection with sh-PAR-1 and pcDNA3.1-PAR-1. The supporting images of the gating strategy are shown in Supplementary Fig. S1D. **C** Statistical results of cell polarisation markers from flow cytometry. One-way ANOVA was used for comparison between multiple groups. n.s, not significant, ****$P < 0.0001$, ***$P < 0.001$ and **$P < 0.01$

[38], rituximab [39], prednisone (R-CHOP) chemoimmunotherapy [40] and cyclophosphamide [41], have greatly improved the treatment, poor prognosis remains a challenge in DLBCL. Thus, it is meaningful to investigate the regulatory mechanisms in the pathogenesis of DLBCL deeply and explore new therapeutic strategies. This study found that rH inhibited M2 macrophage polarisation in a cell model co-cultured with THP-1 and OCI-L10 lymphoma cells and that PAR-1 regulated cell proliferation, migration, invasion and angiogenesis.

Macrophages are vital in regulating tumours and are frequently linked to cancer growth, migration, invasion, and angiogenesis. Macrophages are typically categorised based on the specific cytokines, and M1 and M2 macrophages are two frequently used macrophage phenotypes in current research. The type of polarisation of macrophages is usually linked with a poor prognosis in tumour patients. In tumours, both M1 and M2 are present, except that there is a greater tendency for M1 macrophages to convert to M2 [42]. During tumour development, macrophages undergo a phenotypic transition and eventually become M2 macrophages. Many studies [43–45] have shown that macrophages predominantly exhibit the M2 phenotype in malignant tumours. CD163+is widely used to detect M2 macrophages. In colorectal cancer (CRC) [46], EMT indications were more expressed in clinical samples with high CD163 expression. In this study, we found that M2 macrophage was higher in disease samples by testing 32 clinical samples.

Tumour-associated macrophages (TAMs) have a strong immunomodulatory function, as evidenced by their pivotal involvement in several aspects of tumour development. Some studies illustrate that TAM produces substances that inhibit immune responses, such as IL-10 and IDO metabolites, thereby inhibiting T-cell activation and proliferation [47]. Other studies also demonstrate that TAM promotes angiogenesis and the growth of tumour cells. In lymphomas, TAM is considered an underlying cause. In follicular lymphoma (FL) [48], TAM releases soluble mediators that cause sustained activation of the B cell receptor (BCR). In a model of cutaneous T-cell lymphoma, tumour growth is markedly decelerated with the

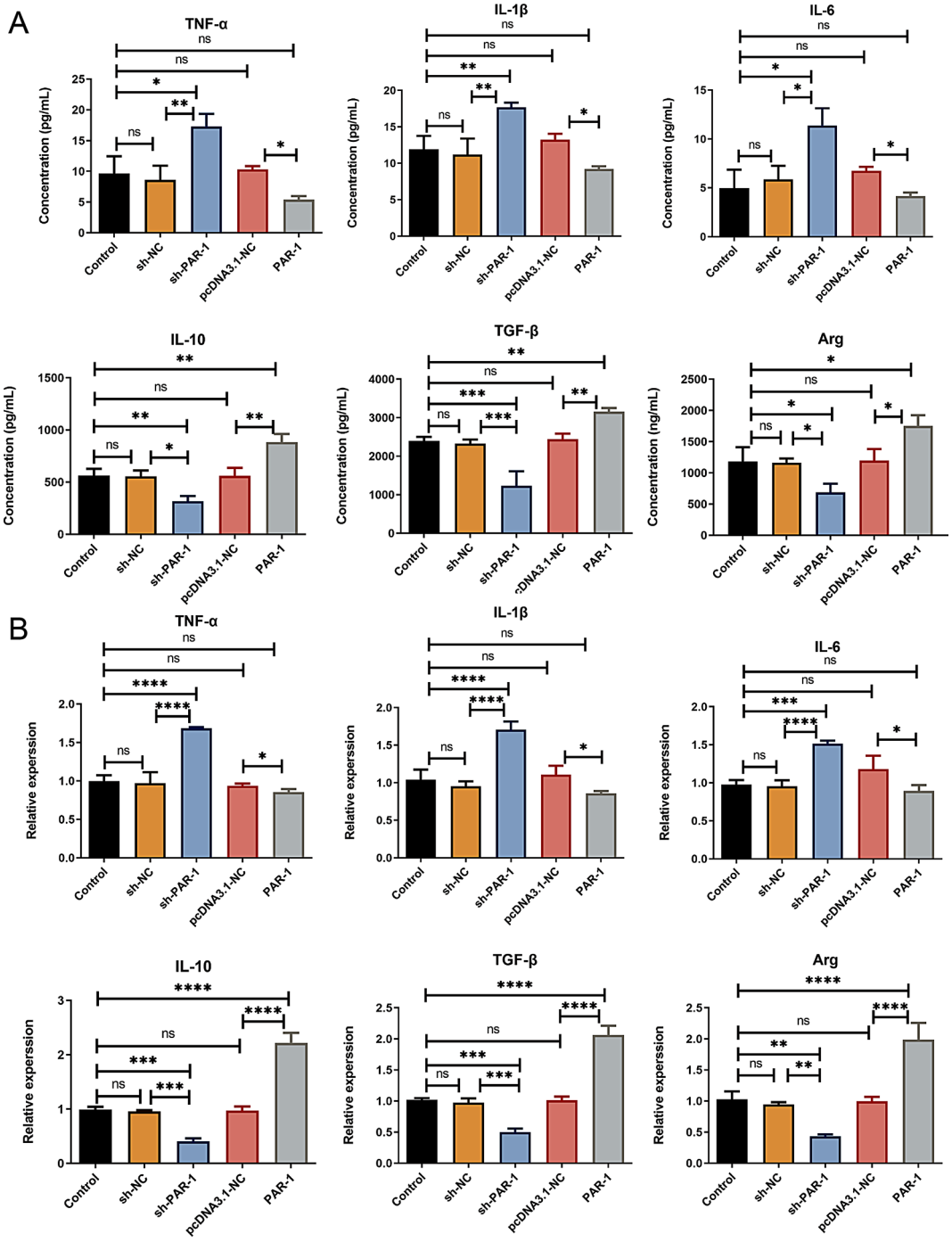

Fig. 6 Effect on M2 macrophage after transfection with sh-PAR-1 and pcDNA3.1-PAR-1. **A** ELISA measured the concentrations of IL-10, TGF-β, Arg, IL-6, TNF-α, and IL-1β. **B** Expression of IL-10, TGF-β, Arg, IL-6, TNF-α, and IL-1β was obtained by RT-qPCR. One-way ANOVA was used for comparison between multiple groups. n.s, not significant, $^{****}P < 0.0001$, $^{***}P < 0.001$, $^{**}P < 0.01$ and $^{*}P < 0.05$

removal of TAM. Many models of macrophage polarisation have been established to study how TAM regulates tumour cells. In HepG2 liver cancer cells [49], A549 lung adenocytes [33], and MCF-7 breast cancer cells [50], models co-cultured with macrophages were established successfully for research. Here, in our article, we refer to the model of the article [51], which is that THP-1 monocyte-induced macrophage co-cultured with tumour cells. Then, we used OCI-Ly10 with THP-1 to establish a model for the analysis of DLBCL. After co-culture, LPS/IFN-γ and IL-4/IL-13 were added to induce M1 and M2 macrophages, respectively. In our experiments, we detected the markers and the levels of cytokines, proving

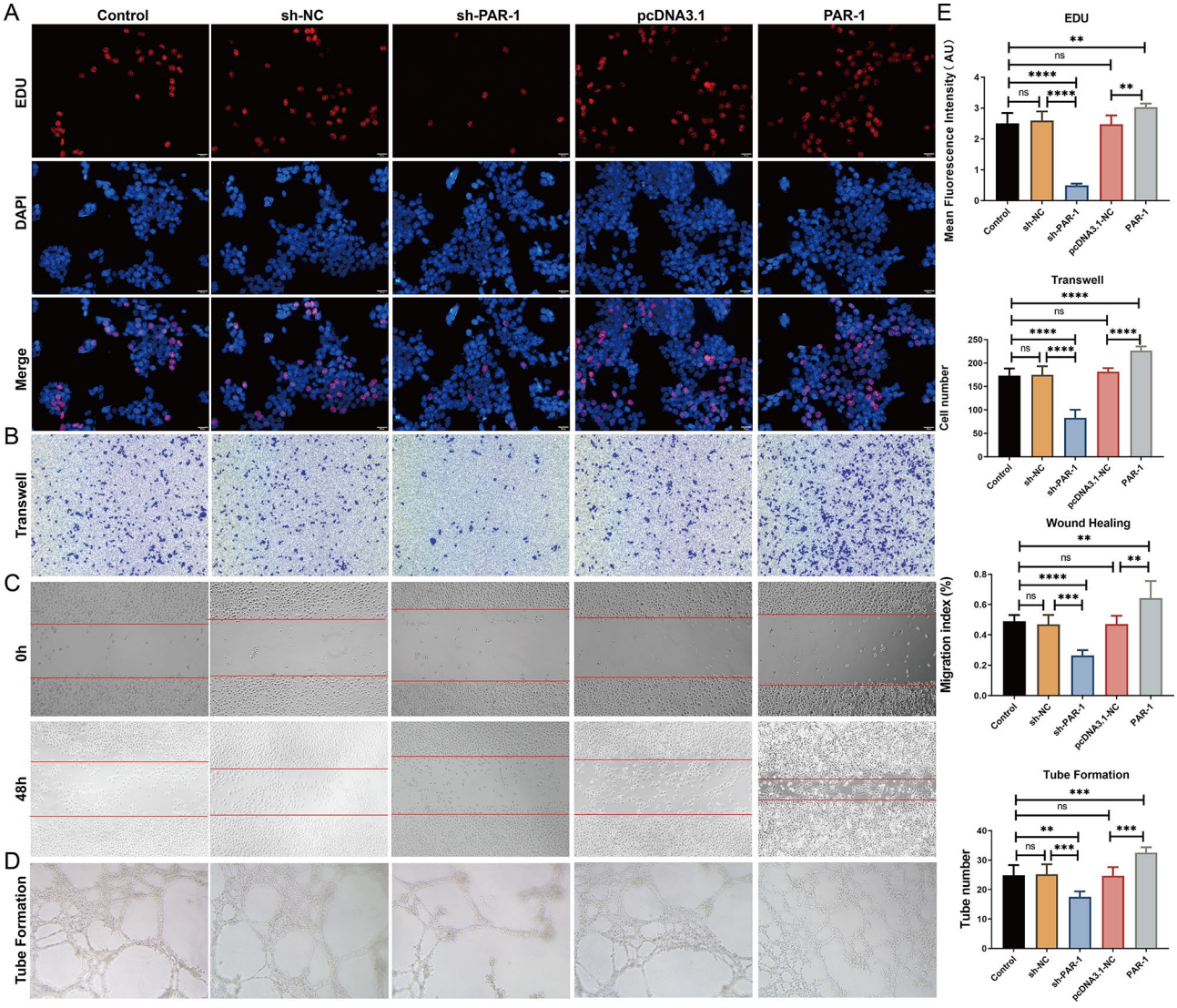

Fig. 7 Regulation of cell viability, migration, invasion and angiogenic capacity by knockdown and overexpression of PAR-1. **A** EDU examined cell viability and found that knockdown of PAR-1 reduced cell viability, with the opposite result for overexpression, scale bar = 20 μm. **B** Transwell assayed the invasive capacity of the cells, and the trend after knockdown and overexpression of PAR-1 was consistent with EDU. **C** A cell wound healing assay tested the migratory capacity of cells and found that PAR-1 regulated the migratory capacity. **D** Angiogenesis experiments demonstrated changes in the number of blood vessels following alterations in PAR-1 expression, x100. One-way ANOVA was used for comparison between multiple groups. n.s, not significant, $^{****}P < 0.0001$, $^{***}P < 0.001$ and $^{**}P < 0.01$

that the cell model was successful, thus continuing with later experiments.

As one of the potent anticoagulants, Hirudin has immense value in tumour-related research. However, due to the limited availability of natural hirudin, recombinant Hirudin (rH) is now used in most studies [52]. In human highly metastatic lung cancer cells (95D), rH was shown to affect the metastasis and invasion of this cell [53]. Research has demonstrated that mitosis in pancreatic cancer cells can be inhibited by Rh [54]. In addition, apoptosis in hepatocellular carcinoma cells (SMMC-7721) was promoted by rH [55]. After successfully establishing the cell model, we added different doses of rH. In DLBCL, we found that rH inhibited the polarization of M2-type macrophages and PAR-1. The article has demonstrated that hirudin ameliorates renal fibrosis by affecting macrophage polarization [30]. In an animal study, hirudin was found to affect inflammatory pathways thereby preventing diabetes-induced kidney damage [56]. Our findings may provide a basis for the therapeutic role of hirudin in DLBCL.

To further investigate the regulatory mechanism in DLBCL, we investigated PAR-1, a promising molecular target in cancer. There is growing evidence [57–60] that it is involved in tumorigenesis and associated with macrophages. PAR-1 overexpression is associated with distal

metastasis of cancer cells in various cancer cell lines [24]. Cancer cells' invasive and migratory capacity is increased after overexpression of PAR-1 [61]. PAR-1 is directly associated with angiogenesis, its expression and VEGF levels [62]. Our article found that PAR-1 is highly expressed in lymphoma M2 macrophages. We used publicly available databases to analyse the expression results of PAR1. The GEPIA database results showed that PAR1 showed high expression in DLBCL ($p<0.05$) (Supplementary Fig. S2E). This is consistent with the finding of high PAR-1 expression in disease samples in clinical samples. We also found that PAR-1 could participate in macrophage polarisation, release of immuno-inflammatory factors and regulation of cell viability, migration, invasion and angiogenesis. Analysis of the correlation between PAR-1 and different macrophage types using online databases gave unsatisfactory results (Supplementary Fig. S2A-D). However, a large number of articles have shown that PAR1 can regulate tumour progression through macrophages and that there is a close link between them [63–65]. The article has been published demonstrating the role of PAR-1 in NHL [25], our study further illustrates that PAR-1 promotes M2 macrophage polarisation and promotes lymphoma cell activity.

Overall, we identified the regulatory role of rH in TAM and the regulatory pathways. However, this proof-of-concept study is missing information about the validation of rH in clinical samples and whether it may affect drug resistance. Additionally, this article lacks information on the combined effects of hirudin and other drugs in DLBCL. It has been suggested that the combination of hirudin and paclitaxel may alleviate the inflammatory response in cardiovascular disease [66, 67]. Rituximab as an effective treatment in non-Hodgkin's lymphoma is a future investigation to be explored regarding whether they can be combined for better therapeutic effects.

Supplementary Information

The online version contains supplementary material available at https://doi.org/10.1186/s12896-024-00879-w.

Supplementary Material 1

Supplementary Material 2

Supplementary Material 3

Acknowledgements
We appreciate our colleagues for their helpful suggestions.

Author contributions
Conceived and designed the experiments: Qiang Pei. Performed the experiments: Zihui Li, Juan Zhao, Jingjing Zhao. Analyzed the data: Haixi Zhang, Tao Qin. Contributed reagents/ materials/analysis tools: Juan Zhao. Writing-original draft: Zihui Li. Writing-review and editing: Qiang Pei.

Funding
This study was supported by the Joint Special Program of Yunnan Province Department and Kunming Medical University for Applied Basic Research (No.201901C070074). The Open project of Yunnan Province Clinical Center for Hematologic Disease (No. 2019LCZXKF-XY10).

Data availability
The datasets used and/or analysed during the current study are available from the corresponding author upon reasonable request.

Declarations

Ethics approval and informed consent to participate
We obey the Helsinki Declaration in clinical data. The study was reported to and approved by The First People's Hospital of Yunnan Province Ethics Committee (YYLH052). Informed consent was signed for information collection. We state that we obtained informed consent signed by all participants including 32 participants.

Consent for publication
Not applicable.

Competing interests
The authors declare no competing interests.

Received: 20 January 2024 / Accepted: 22 July 2024
Published online: 12 August 2024

References

1. Schmitz R, Wright GW, Huang DW, Johnson CA, Phelan JD, Wang JQ, Roulland S, Kasbekar M, Young RM, Shaffer AL, et al. Genetics and Pathogenesis of diffuse large B-Cell lymphoma. N Engl J Med. 2018;378(15):1396–407.
2. Marcus R, Hagenbeek A. The therapeutic use of rituximab in non-Hodgkin's lymphoma. Eur J Haematol Suppl 2007(67):5–14.
3. Keane C, Tobin J, Gunawardana J, Francis S, Gifford G, Gabrielli S, Gill A, Stevenson W, Talaulikar D, Gould C, et al. The tumour microenvironment is immuno-tolerogenic and a principal determinant of patient outcome in EBV-positive diffuse large B-cell lymphoma. Eur J Haematol. 2019;103(3):200–7.
4. Gordon S, Plüddemann A, Martinez Estrada F. Macrophage heterogeneity in tissues: phenotypic diversity and functions. Immunol Rev. 2014;262(1):36–55.
5. Yang N, Liu Y. The role of the Immune Microenvironment in Bone Regeneration. Int J Med Sci 2021, 18(16):3697–707.
6. Wang M, Pan W, Xu Y, Zhang J, Wan J, Jiang H. Microglia-mediated neuroinflammation: a potential target for the treatment of Cardiovascular diseases. J Inflamm Res. 2022;15:3083–94.
7. Gordon S. Alternative activation of macrophages. Nat Rev Immunol. 2003;3(1):23–35.
8. Liu W, Yu M, Xie D, Wang L, Ye C, Zhu Q, Liu F, Yang L. Melatonin-stimulated MSC-derived exosomes improve diabetic wound healing through regulating macrophage M1 and M2 polarization by targeting the PTEN/AKT pathway. Stem Cell Res Ther. 2020;11(1):259.
9. Bardi GT, Smith MA, Hood JL. Melanoma exosomes promote mixed M1 and M2 macrophage polarization. Cytokine. 2018;105:63–72.
10. Gerasimova EV, Popkova TV, Gerasimova DA, Kirichenko TV. Macrophage dysfunction in Autoimmune Rheumatic diseases and atherosclerosis. Int J Mol Sci 2022, 23(9).
11. Wang C, Ma C, Gong L, Guo Y, Fu K, Zhang Y, Zhou H, Li Y. Macrophage polarization and its role in Liver Disease. Front Immunol. 2021;12:803037.
12. Wu H, Zheng J, Xu S, Fang Y, Wu Y, Zeng J, Shao A, Shi L, Lu J, Mei S, et al. Mer regulates microglial/macrophage M1/M2 polarization and alleviates neuroinflammation following traumatic brain injury. J Neuroinflamm. 2021;18(1):2.
13. Lin R, Chen X, Su F, Wang H, Han B, Chen Y, Zhang C, Ma M. The germline HLA-A02B62 supertype is associated with a PD-L1-positive tumour immune microenvironment and poor prognosis in stage I lung cancer. Heliyon. 2023;9(8):e18948.
14. Lahmar Q, Keirsse J, Laoui D, Movahedi K, Van Overmeire E, Van Ginderachter JA. Tissue-resident versus monocyte-derived macrophages in the tumor microenvironment. Biochim Biophys Acta. 2016;1865(1):23–34.
15. Boutilier AJ, Elsawa SF. Macrophage polarization States in the Tumor Microenvironment. Int J Mol Sci 2021, 22(13).
16. Zhao S, Mi Y, Guan B, Zheng B, Wei P, Gu Y, Zhang Z, Cai S, Xu Y, Li X, et al. Tumor-derived exosomal miR-934 induces macrophage M2 polarization

to promote liver metastasis of colorectal cancer. J Hematol Oncol. 2020;13(1):156.
17. Kanlikilicer P, Bayraktar R, Denizli M, Rashed MH, Ivan C, Aslan B, Mitra R, Karagoz K, Bayraktar E, Zhang X, et al. Exosomal miRNA confers chemo resistance via targeting Cav1/p-gp/M2-type macrophage axis in ovarian cancer. EBioMedicine. 2018;38:100–12.
18. Zong S, Dai W, Guo X, Wang K. LncRNA-SNHG1 promotes macrophage M2-like polarization and contributes to breast cancer growth and metastasis. Aging. 2021;13(19):23169–81.
19. Liu M, Bertolazzi G, Sridhar S, Lee RX, Jaynes P, Mulder K, Syn N, Hoppe MM, Fan S, Peng Y, et al. Spatially-resolved transcriptomics reveal macrophage heterogeneity and prognostic significance in diffuse large B-cell lymphoma. Nat Commun. 2024;15(1):2113.
20. Zhang Y, Xiang J, Sheng X, Zhu N, Deng S, Chen J, Yu L, Zhou Y, Lin C, Shen J. GM-CSF enhanced the effect of CHOP and R-CHOP on inhibiting diffuse large B-cell lymphoma progression via influencing the macrophage polarization. Cancer Cell Int. 2021;21(1):141.
21. Nierodzik ML, Karpatkin S. Thrombin induces tumor growth, metastasis, and angiogenesis: evidence for a thrombin-regulated dormant tumor phenotype. Cancer Cell. 2006;10(5):355–62.
22. Morris DR, Ding Y, Ricks TK, Gullapalli A, Wolfe BL, Trejo J. Protease-activated receptor-2 is essential for factor VIIa and Xa-induced signaling, migration, and invasion of breast cancer cells. Cancer Res. 2006;66(1):307–14.
23. Saleiban A, Faxälv L, Claesson K, Jönsson JI, Osman A. miR-20b regulates expression of proteinase-activated receptor-1 (PAR-1) thrombin receptor in melanoma cells. Pigment cell Melanoma Res. 2014;27(3):431–41.
24. Otsuki T, Fujimoto D, Hirono Y, Goi T, Yamaguchi A. Thrombin conducts epithelial–mesenchymal transition via protease–activated receptor–1 in human gastric cancer. Int J Oncol. 2014;45(6):2287–94.
25. Schiller H, Bartscht T, Arlt A, Zahn MO, Seifert A, Bruhn T, Bruhn HD, Gieseler F. Thrombin as a survival factor for cancer cells: thrombin activation in malignant effusions in vivo and inhibition of idarubicin-induced cell death in vitro. Int J Clin Pharmacol Ther. 2002;40(8):329–35.
26. Liu X, Yu J, Song S, Yue X, Li Q. Protease-activated receptor-1 (PAR-1): a promising molecular target for cancer. Oncotarget. 2017;8(63):107334–45.
27. Green D, Karpatkin S. Role of thrombin as a tumor growth factor. Cell Cycle (Georgetown Tex). 2010;9(4):656–61.
28. Hernández-Rodríguez NA, Correa E, Contreras-Paredes A, Green L. Evidence that thrombin present in lungs of patients with pulmonary metastasis may contribute to the development of the disease. Lung cancer (Amsterdam Netherlands). 1999;26(3):157–67.
29. Lu Q, Lv M, Xu E, Shao F, Feng Y, Yang J, Shi L. Recombinant hirudin suppresses the viability, adhesion, migration and invasion of Hep-2 human laryngeal cancer cells. Oncol Rep. 2015;33(3):1358–64.
30. Chen B, Ding X, Yang Y. Hirudin Regulates Vascular Function in Chronic Renal Failure through Modulating Macrophage Polarization. BioMed research international 2022, 2022:6043698.
31. Kou J, Gao L, Ni L, Shao T, Ding J. Mechanism of hirudin-mediated inhibition of Proliferation in Ovarian Cancer cells. Molecular biotechnology 2024.
32. Zhao B, Wu M, Hu Z, Ma Y, Qi W, Zhang Y, Li Y, Yu M, Wang H, Mo W. Thrombin is a therapeutic target for non-small-cell lung cancer to inhibit vasculogenic mimicry formation. Signal Transduct Target Therapy. 2020;5(1):117.
33. Xu F, Cui WQ, Wei Y, Cui J, Qiu J, Hu LL, Gong WY, Dong JC, Liu BJ. Astragaloside IV inhibits lung cancer progression and metastasis by modulating macrophage polarization through AMPK signaling. J Exp Clin Cancer Res. 2018;37(1):207.
34. Le Fournis C, Jeanneau C, Giraud T, El Karim I, Lundy FT, About I. Fibroblasts control macrophage differentiation during pulp inflammation. J Endod. 2021;47(9):1427–34.
35. Varghese F, Bukhari AB, Malhotra R, De A. IHC profiler: an open source plugin for the quantitative evaluation and automated scoring of immunohistochemistry images of human tissue samples. PLoS ONE. 2014;9(5):e96801.
36. Mohamed O, El Bastawisy A, Allahlobi N, Abdellateif MS, Zekri ARN, Shaarawy S, Korany Z, Mohanad M, Bahnassy AA. The role of CD68 + macrophage in classical Hodgkin lymphoma patients from Egypt. Diagn Pathol. 2020;15(1):10.
37. Mishra M, Tiwari S, Gomes AV. Protein purification and analysis: next generation Western blotting techniques. Expert Rev Proteom 2017, 14(11):1037–53.
38. van der Horst HJ, de Jonge AV, Hiemstra IH, Gelderloos AT, Berry D, Hijmering NJ, van Essen HF, de Jong D, Chamuleau MED, Zweegman S, et al. Epcoritamab induces potent anti-tumor activity against malignant B-cells from patients with DLBCL, FL and MCL, irrespective of prior CD20 monoclonal antibody treatment. Blood cancer J. 2021;11(2):38.
39. Sehn LH, Hertzberg M, Opat S, Herrera AF, Assouline S, Flowers CR, Kim TM, McMillan A, Ozcan M, Safar V, et al. Polatuzumab vedotin plus bendamustine and rituximab in relapsed/refractory DLBCL: survival update and new extension cohort data. Blood Adv. 2022;6(2):533–43.
40. Coiffier B, Sarkozy C. Diffuse large B-cell lymphoma: R-CHOP failure-what to do? Hematology American Society of Hematology Education Program 2016, 2016(1):366–78.
41. Kambhampati S, Saumoy M, Schneider Y, Pak S, Budde LE, Mei MG, Siddiqi T, Popplewell LL, Wen YP, Zain J, et al. Cost-effectiveness of polatuzumab vedotin combined with chemoimmunotherapy in untreated diffuse large B-cell lymphoma. Blood. 2022;140(25):2697–708.
42. Pan Y, Yu Y, Wang X, Zhang T. Tumor-Associated macrophages in Tumor Immunity. Front Immunol. 2020;11:583084.
43. Mantovani A, Sozzani S, Locati M, Allavena P, Sica A. Macrophage polarization: tumor-associated macrophages as a paradigm for polarized M2 mononuclear phagocytes. Trends Immunol. 2002;23(11):549–55.
44. Biswas SK, Gangi L, Paul S, Schioppa T, Saccani A, Sironi M, Bottazzi B, Doni A, Vincenzo B, Pasqualini F, et al. A distinct and unique transcriptional program expressed by tumor-associated macrophages (defective NF-kappaB and enhanced IRF-3/STAT1 activation). Blood. 2006;107(5):2112–22.
45. Saccani A, Schioppa T, Porta C, Biswas SK, Nebuloni M, Vago L, Bottazzi B, Colombo MP, Mantovani A, Sica A. p50 nuclear factor-kappab overexpression in tumor-associated macrophages inhibits M1 inflammatory responses and antitumor resistance. Cancer Res. 2006;66(23):11432–40.
46. Wei C, Yang C, Wang S, Shi D, Zhang C, Lin X, Liu Q, Dou R, Xiong B. Crosstalk between cancer cells and tumor associated macrophages is required for mesenchymal circulating tumor cell-mediated colorectal cancer metastasis. Mol Cancer. 2019;18(1):64.
47. Campesato LF, Budhu S, Tchaicha J, Weng CH, Gigoux M, Cohen IJ, Redmond D, Mangarin L, Pourpe S, Liu C, et al. Blockade of the AHR restricts a Treg-macrophage suppressive axis induced by L-Kynurenine. Nat Commun. 2020;11(1):4011.
48. Andor N, Simonds EF, Czerwinski DK, Chen J, Grimes SM, Wood-Bouwens C, Zheng GXY, Kubit MA, Greer S, Weiss WA, et al. Single-cell RNA-Seq of follicular lymphoma reveals malignant B-cell types and coexpression of T-cell immune checkpoints. Blood. 2019;133(10):1119–29.
49. Wan S, Zhao E, Kryczek I, Vatan L, Sadovskaya A, Ludema G, Simeone DM, Zou W, Welling TH. Tumor-associated macrophages produce interleukin 6 and signal via STAT3 to promote expansion of human hepatocellular carcinoma stem cells. Gastroenterology. 2014;147(6):1393–404.
50. Jain RK. Normalization of tumor vasculature: an emerging concept in antiangiogenic therapy. Sci (New York NY). 2005;307(5706):58–62.
51. Genin M, Clement F, Fattaccioli A, Raes M, Michiels C. M1 and M2 macrophages derived from THP-1 cells differentially modulate the response of cancer cells to etoposide. BMC Cancer. 2015;15:577.
52. Li T, Ma J, Xu Z, Wang S, Wang N, Shao S, Yang W, Huang L, Liu Y. Transcriptomic Analysis of the Influence of Methanol Assimilation on the Gene Expression in the Recombinant Pichia pastoris Producing Hirudin Variant 3. Genes 2019, 10(8).
53. Yi S, Niu D, Bai F, Li S, Huang L, He W, Prasad A, Czachor A, Tan LC, Kolliputi N, et al. Soluble expression of a human MnSOD and Hirudin Fusion Protein in Escherichia coli, and its effects on Metastasis and Invasion of 95-D cells. J Microbiol Biotechnol. 2016;26(11):1881–90.
54. Ferrer-Miralles N, Domingo-Espín J, Corchero JL, Vázquez E, Villaverde A. Microbial factories for recombinant pharmaceuticals. Microb Cell Fact. 2009;8:17.
55. Fischer KG. The role of recombinant hirudins in the management of thrombotic disorders. BioDrugs: Clin Immunotherapeutics Biopharmaceuticals gene Therapy. 2004;18(4):235–68.
56. Han J, Pang X, Zhang Y, Peng Z, Shi X, Xing Y. Hirudin protects against kidney damage in Streptozotocin-Induced Diabetic Nephropathy rats by inhibiting inflammation via P38 MAPK/NF-κB pathway. Drug Des Devel Ther. 2020;14:3223–34.
57. Zigler M, Kamiya T, Brantley EC, Villares GJ, Bar-Eli M. PAR-1 and thrombin: the ties that bind the microenvironment to melanoma metastasis. Cancer Res. 2011;71(21):6561–6.
58. Villares GJ, Zigler M, Bar-Eli M. The emerging role of the thrombin receptor (PAR-1) in melanoma metastasis–a possible therapeutic target. Oncotarget. 2011;2(1–2):8–17.

59. Tatour M, Shapira M, Axelman E, Ghanem S, Keren-Politansky A, Bonstein L, Brenner B, Nadir Y. Thrombin is a selective inducer of heparanase release from platelets and granulocytes via protease-activated receptor-1. Thromb Haemost. 2017;117(7):1391–401.
60. Kim SJ, Shin JY, Lee KD, Bae YK, Choi IJ, Park SH, Chun KH. Galectin-3 facilitates cell motility in gastric cancer by up-regulating protease-activated receptor-1 (PAR-1) and matrix metalloproteinase-1 (MMP-1). PLoS ONE. 2011;6(9):e25103.
61. Borensztajn KS, Bijlsma MF, Groot AP, Brüggemann LW, Versteeg HH, Reitsma PH, Peppelenbosch MP, Spek CA. Coagulation factor xa drives tumor cells into apoptosis through BH3-only protein bim up-regulation. Exp Cell Res. 2007;313(12):2622–33.
62. Villares GJ, Zigler M, Wang H, Melnikova VO, Wu H, Friedman R, Leslie MC, Vivas-Mejia PE, Lopez-Berestein G, Sood AK, et al. Targeting melanoma growth and metastasis with systemic delivery of liposome-incorporated protease-activated receptor-1 small interfering RNA. Cancer Res. 2008;68(21):9078–86.
63. Tekin C, Aberson HL, Waasdorp C, Hooijer GKJ, de Boer OJ, Dijk F, Bijlsma MF, Spek CA. Macrophage-secreted MMP9 induces mesenchymal transition in pancreatic cancer cells via PAR1 activation. Cell Oncol (Dordrecht). 2020;43(6):1161–74.
64. Hwang YS, Cho HJ, Park ES, Lim J, Yoon HR, Kim JT, Yoon SR, Jung H, Choe YK, Kim YH et al. KLK6/PAR1 Axis promotes Tumor Growth and Metastasis by regulating cross-talk between Tumor cells and macrophages. Cells 2022, 11(24).
65. Healy LD, Fernández JA, Mosnier LO, Griffin JH. Activated protein C and PAR1-derived and PAR3-derived peptides are anti-inflammatory by suppressing macrophage NLRP3 inflammasomes. J Thromb Haemostasis: JTH. 2021;19(1):269–80.
66. Li H, Wang X, Xu A. Effect of paclitaxel + hirudin on the TLR4-MyD88 signaling pathway during inflammatory activation of human coronary artery smooth muscle cells and mechanistic analysis. Cell Physiol Biochemistry: Int J Experimental Cell Physiol Biochem Pharmacol. 2018;50(4):1301–17.
67. Wang X, Li H, Sun X, Wang X, Wang G. Evaluation of drug release from paclitaxel + hirudin-eluting balloons and the resulting vascular reactivity in healthy pigs. Experimental Therapeutic Med. 2018;16(4):3425–32.

Publisher's Note